

# Combining Left and Right Palmprint Images for More Accurate Personal Identification

Yong Xu, *Member, IEEE*, Lunke Fei, and David Zhang, *Fellow, IEEE*

**Abstract**—Multibiometrics can provide higher identification accuracy than single biometrics, so it is more suitable for some real-world personal identification applications that need high-standard security. Among various biometrics technologies, palmprint identification has received much attention because of its good performance. Combining the left and right palmprint images to perform multibiometrics is easy to implement and can obtain better results. However, previous studies did not explore this issue in depth. In this paper, we proposed a novel framework to perform multibiometrics by comprehensively combining the left and right palmprint images. This framework integrated three kinds of scores generated from the left and right palmprint images to perform matching score-level fusion. The first two kinds of scores were, respectively, generated from the left and right palmprint images and can be obtained by any palmprint identification method, whereas the third kind of score was obtained using a specialized algorithm proposed in this paper. As the proposed algorithm carefully takes the nature of the left and right palmprint images into account, it can properly exploit the similarity of the left and right palmprints of the same subject. Moreover, the proposed weighted fusion scheme allowed perfect identification performance to be obtained in comparison with previous palmprint identification methods.

**Index Terms**—Palmprint recognition, biometrics, multi-biometrics.

## I. INTRODUCTION

**P**ALMPRINT identification is an important personal identification technology and it has attracted much attention. The palmprint contains not only principle curves and wrinkles but also rich texture and miniscule points, so the palmprint identification is able to achieve a high accuracy because of available rich information in palmprint [1]–[8].

Various palmprint identification methods, such as coding based methods [5]–[9] and principle curve methods [10], have been proposed in past decades. In addition to these methods, subspace based methods can also

perform well for palmprint identification. For example, Eigenpalm and Fisherpalm [11]–[14] are two well-known subspace based palmprint identification methods. In recent years, 2D appearance based methods such as 2D Principal Component Analysis (2DPCA) [15], 2D Linear Discriminant Analysis (2DLDA) [16], and 2D Locality Preserving Projection (2DLPP) [17] have also been used for palmprint recognition. Further, the Representation Based Classification (RBC) method also shows good performance in palmprint identification [18]. Additionally, the Scale Invariant Feature Transform (SIFT) [19], [20], which transforms image data into scale-invariant coordinates, are successfully introduced for the contactless palmprint identification.

No single biometric technique can meet all requirements in circumstances [21]. To overcome the limitation of the unimodal biometric technique and to improve the performance of the biometric system, multimodal biometric methods are designed by using multiple biometrics or using multiple modals of the same biometric trait, which can be fused at four levels: image (sensor) level, feature level, matching score level and decision level [22]–[25]. For the image level fusion, Han et al. [26] proposed a multispectral palmprint recognition method in which the palmprint images were captured under Red, Green, Blue, and Infrared illuminations and a wavelet-based image fusion method is used for palmprint recognition. Examples of fusion at feature level include the combination of and integration of multiple biometric traits. For example, Kumar et al. [27] improved the performance of palmprint-based verification by integrating hand geometry features. In [28] and [29], the face and palmprint were integrated for personal identification. For the fusion at matching score level, various kinds of methods are also proposed. For instance, Zhang et al. [30] designed a joint palmprint and palmvein fusion system for personal identification. Dai et al. [31] proposed a weighted sum rule to fuse the palmprint minutiae, density, orientation and principal lines for the high resolution palmprint verification and identification. Particularly, Morales et al. [20] proposed a combination of two kinds of matching scores obtained by multiple matchers, the SIFT and orthogonal line ordinal features (OLOF), for contactless palmprint identification. One typical example of the decision level fusion on palmprint is that Kumar et al. [32] fused three major palmprint representations at the decision level.

Conventional multimodal biometrics methods treat different traits independently. However, some special kinds of biometric traits have a similarity and these methods cannot exploit the similarity of different kinds of traits. For example, the left and right palmprint traits of the same subject can be viewed as

Manuscript received April 18, 2014; revised August 16, 2014 and November 2, 2014; accepted December 4, 2014. Date of publication December 18, 2014; date of current version January 8, 2015. This work was supported in part by the National Natural Science Foundation of China under Grant 61370163, Grant 61233011, and Grant 61332011, and in part by the Shenzhen Municipal Science and Technology Innovation Council under Grant JCYJ20130329151843309 and Grant JCYJ20130329151843309. The associate editor coordinating the review of this manuscript and approving it for publication was Prof. Shiguang Shan.

Y. Xu and L. Fei are with the Research Center of Biocomputing, Harbin Institute of Technology Shenzhen Graduate School, Shenzhen 518055, China (e-mail: laterfall2@yahoo.com.cn; flksxm@126.com).

D. Zhang is with the Biometrics Research Centre, Department of Computing, The Hong Kong Polytechnic University, Hong Kong (e-mail: csdzhang@comp.polyu.edu.hk).

Color versions of one or more of the figures in this paper are available online at <http://ieeexplore.ieee.org>.

Digital Object Identifier 10.1109/TIP.2014.2380171

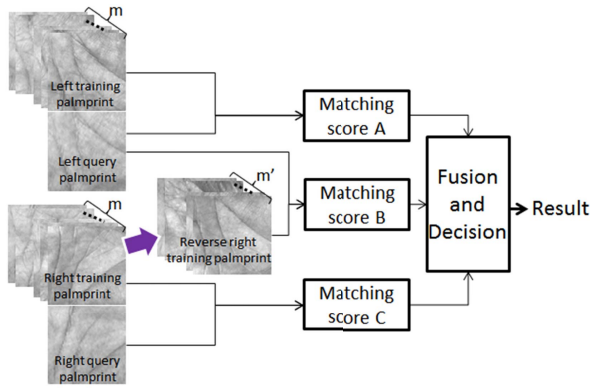


Fig. 1. Procedures of the proposed framework.

this kind of special biometric traits owing to the similarity between them, which will be demonstrated later. However, there is almost no any attempt to explore the correlation between the left and right palmprint and there is no “special” fusion method for this kind of biometric identification. In this paper, we propose a novel framework of combining the left with right palmprint at the matching score level. Fig. 1 shows the procedure of the proposed framework. In the framework, three types of matching scores, which are respectively obtained by the left palmprint matching, right palmprint matching and crossing matching between the left query and right training palmprint, are fused to make the final decision. The framework not only combines the left and right palmprint images for identification, but also properly exploits the similarity between the left and right palmprint of the same subject. Extensive experiments show that the proposed framework can integrate most conventional palmprint identification methods for performing identification and can achieve higher accuracy than conventional methods.

This work has the following notable contributions. First, it for the first time shows that the left and right palmprint of the same subject are somewhat correlated, and it demonstrates the feasibility of exploiting the crossing matching score of the left and right palmprint for improving the accuracy of identity identification. Second, it proposes an elaborated framework to integrate the left palmprint, right palmprint, and crossing matching of the left and right palmprint for identity identification. Third, it conducts extensive experiments on both touch-based and contactless palmprint databases to verify the proposed framework.

The remainder of the paper is organized as follows: Section II briefly presents previous palmprint identification methods. Section III describes the proposed framework. Section IV reports the experimental results and Section V offers the conclusion of the paper.

## II. PREVIOUS WORK

Generally speaking, the principal lines and texture are two kinds of salient features of palmprint. The principal line based methods and coding based methods have been widely used in palmprint identification. In addition, sub-space based methods,

representation based methods and SIFT based methods can also be applied for palmprint identification.

### A. Line Based Method

Lines are the basic feature of palmprint and line based methods play an important role in palmprint verification and identification. Line based methods use lines or edge detectors to extract the palmprint lines and then use them to perform palmprint verification and identification. In general, most palms have three principal lines: the heartline, headline, and lifeline, which are the longest and widest lines in the palmprint image and have stable line shapes and positions. Thus, the principal line based method is able to provide stable performance for palmprint verification.

Palmprint principal lines can be extracted by using the Gabor filter, Sobel operation, or morphological operation. In this paper, the Modified Finite Radon Transform (MFRAT) method [10] is used to extract the principal lines of the palmprint. The pixel-to-area matching strategy is adopted for principal lines matching in Robust Line Orientation Code (RLOC) method [33], which defines a principal lines matching score as follows:

$$S(A, B) = \left( \sum_{i=1}^m \sum_{j=1}^n A(i, j) \& \bar{B}(i, j) \right) / N_A, \quad (1)$$

where  $A$  and  $B$  are two palmprint principal lines images, “&” represents the logical “AND” operation,  $N_A$  is the number of pixel points of  $A$ , and  $\bar{B}(i, j)$  represents a neighbor area of  $B(i, j)$ . For example,  $\bar{B}(i, j)$  can be defined as a set of five pixel points,  $B(i-1, j)$ ,  $B(i+1, j)$ ,  $B(i, j)$ ,  $B(i, j-1)$ , and  $B(i, j+1)$ . The value of  $A(i, j) \& \bar{B}(i, j)$  will be 1 if  $A(i, j)$  and at least one of  $\bar{B}(i, j)$  are simultaneously principal lines points, otherwise, the value of  $A(i, j) \& \bar{B}(i, j)$  is 0.  $S(A, B)$  is between 0 and 1, and the larger the matching score is, the more similar  $A$  and  $B$  are. Thus, the query palmprint can be classified into the class that produces the maximum matching score.

### B. Coding Based Method

Coding based methods are the most influential palmprint identification methods [5]–[9]. Representative coding based methods include the competitive code method, ordinal code method, palmcode method and Binary Orientation Co-occurrence Vector (BOCV) method [34], and so on.

The competitive code method [6] uses six Gabor filters with six different directions  $\theta_j = j\pi/6$ ,  $j \in \{0, 1, \dots, 5\}$ , to extract orientation features from the palmprint as follows. Six directional Gabor templates are convoluted with the palmprint image respectively. The dominant direction is defined as the direction with the greatest response, the index  $j$  ( $j = 0 \dots 5$ ) of which is indicated as the competitive code.

In the matching stage of the competitive code method, the matching score between two palmprint images is calculated by using the angular distance, which can be defined as:

$$S_D = \frac{1}{3N^2} \sum_{i=1}^N \sum_{j=1}^N F(D_d(i, j), D_t(i, j)), \quad (2)$$

where  $Dd$  and  $Dt$  be two index code planes of two palmprint images and  $F(\alpha, \beta) = \min(|\alpha - \beta|, 6 - |\alpha - \beta|)$ . The  $N$  is the number of the pixels of the palmprint image.  $S_D$  is in the range of 0 to 1. The smaller the  $S_D$  is, the more similar the two samples are.

The competitive code can be represented by three bit binary codes according to the rule of [6]. Then the Hamming distance can be used to measure the similarity between two competitive codes, which can be calculated by:

$$D(P, Q) = \frac{\sum_{y=1}^N \sum_{x=1}^N \sum_{i=1}^3 (P_i(x, y) \otimes Q_i(x, y))}{3N^2}, \quad (3)$$

where  $P_i(Q_i)$  is the  $i$ th bit binary code plane. “ $\otimes$ ” is the logical “XOR” operation. The smaller the Hamming distance (angular distance) is, the more similar the two samples are. Therefore, the query palmprint is assigned to the class that produces the smallest angular distance.

Differing from the competitive code method, the palmcode method [5] uses only one optimized 2D Gabor filter with direction of  $\pi/4$  to extract palmprint texture features. Then it uses a feature vector to represent image data that consists of a real part feature and an imaginary part feature. Finally it employs a normalized Hamming distance to calculate the matching score of two palmprint feature vectors. In the ordinal code method [8], three integrated filters, each of which is composed of two perpendicular 2D Gaussian filters, are employed to convolute a palmprint image and three bit ordinal codes are obtained based on the sign of filtering results. Then the Hamming distance is used to calculate the matching score of two palmprint ordinal codes. In the fusion code method [9] multiple elliptical Gabor filters with four different directions are convoluted with palmprint images, and then the direction and phase information of the responses are encoded into a pair of binary codes, which are exploited to calculate the normalized Hamming distance for palmprint verification. In the BOCV method, the same six filters as the competitive code method are convoluted with the palmprint image, respectively. All six orientation features are encoded as six binary codes successively, which are joined to calculate the Hamming distance between the query palmprint and the gallery palmprint. The Sparse Multiscale Competitive Code (SMCC) method [7] adopts a bank of Derivatives of Gaussians (DoG) filters with different scales and orientations to obtain the multiscale orientation features by using the  $l_1$ -norm sparse coding algorithm. The same coding rule as the competitive code method is adopted to integrate the feature with the dominant orientation into the SMCC code and finally the angular distance is calculated for the gallery SMCC code and the query SMCC code in the matching stage.

### C. Subspace Based Methods

Subspace based methods include the PCA, LDA, and ICA etc. The key idea behind PCA is to find an orthogonal subspace that preserves the maximum variance of the original data. The PCA method tries to find the best set of projection directions in the sample space that will maximize the total scatter across

all samples by using the following objective function:

$$J_{PCA} = \arg \max_W |W^T S_t W|, \quad (4)$$

where  $S_t$  is the total scatter matrix of the training samples, and  $W$  is the projection matrix whose columns are orthonormal vectors. PCA chooses the first few principal components and uses them to transform the samples in to a low-dimensional feature space.

LDA tries to find an optimal projection matrix  $W$  and transforms the original space to a lower-dimensional feature space. In the low dimensional space, LDA not only maximizes the Euclidean distance of samples from different classes but also minimizes the distance of samples from the same classes. As a result, the goal of LDA is to maximize the ratio of the between-class distance against within-class distance which is defined as:

$$J_{LDA} = \arg \max_W \frac{|W^T S_b W|}{|W^T S_w W|}, \quad (5)$$

where  $S_b$  is the between-class scatter matrix, and  $S_w$  is the within-class scatter matrix. In the subspace palmprint identification method, the query palmprint image is usually classified into the class which produces the minimum Euclidean distance with the query sample in the low-dimensional feature space.

### D. Representation Based Method

The representation based method uses training samples to represent the test sample, and selects a candidate class with the maximum contribution to the test sample. The Collaborative Representation based Classification (CRC) method, Sparse Representation-Based Classification (SRC) method and Two-Phase Test Sample Sparse Representation (TPTSSR) method are two representative representation based methods [35], [36]. Almost all representation based methods can be easily applied to perform palmprint identification. The CRC method uses all training samples to represent the test sample. Assuming that there are  $C$  classes and  $n$  training samples  $x_1 x_2 \dots x_n$ , CRC expresses the test sample as:

$$y = a_1 x_1 + a_2 x_2 + \dots + a_n x_n, \quad (6)$$

where  $y$  is the test sample, and  $a_i$  ( $i = 1, 2, \dots, n$ ) is the weight coefficient. It can be rewritten as  $y = XA$ , where  $A = [a_1 a_2 \dots a_n]^T$ ,  $X = [x_1 x_2 \dots x_n]$ .  $x_1 x_2 \dots x_n$  and  $y$  are all column vectors. If  $X$  is nonsingular,  $A$  can be obtained by using  $A = X^{-1}y$ . If  $X$  is singular,  $A$  can be obtained by using  $A = (X^T X + \delta I)^{-1} X^T y$ , where  $\delta$  is a small positive constant and  $I$  is the identity matrix. The contribution of the  $i$ th training sample to representing the test sample is  $a_i x_i$ . So the sum of the contribution from the  $j$ th class is  $s_j = a_{j_1} x_{j_1} + a_{j_2} x_{j_2} + \dots + a_{j_n} x_{j_n}$ ,  $j_k$  ( $k = 1, 2, \dots$ ) is the sequence number of the  $k$ th training sample from the  $j$ th class. The deviation of  $s_j$  from  $y$  can be calculated using

$$e_j = \|y - (a_{j_1} x_{j_1} + a_{j_2} x_{j_2} + \dots + a_{j_n} x_{j_n})\|^2, \quad j \in C. \quad (7)$$

A smaller deviation  $e_j$  means a greater contribution to representing the test sample. Thus,  $y$  can be classified into the class  $q$  that produces the smallest deviation.

The TPTSSR method was proposed in 2011 and it has performed well in face recognition and palmprint identification [37]. The method first determines  $M$  nearest neighbor training samples for the test sample. Then it uses the determined  $M$  neighbor training samples to represent the test sample, and selects the class with the greatest contribution to representing the query sample as the class to which the query sample belongs.

### E. SIFT Based Method

SIFT was originally proposed in [19] for object classification applications, which are introduced for contactless palmprint identification in recent years [20], [38]. Because the contactless palmprint images have severe variations in poses, scales, rotations and translations, which make conventional palmprint feature extraction methods on contactless imaging schemes questionable and therefore, the identification accuracy of conventional palmprint recognition methods is usually not satisfactory for contactless palmprint identification. The features extracted by SIFT are invariant to image scaling, rotation and partially invariant to the change of projection and illumination. Therefore, the SIFT based method is insensitive to the scaling, rotation, projective and illumination factors, and thus is advisable for the contactless palmprint identification.

The SIFT based method firstly searches over all scales and image locations by using a difference-of-Gaussian function to identify potential interest points. Then an elaborated model is used to determine finer location and scale at each candidate location and keypoints are selected based on the stability. Then one or more orientations are assigned to each keypoint location based on local image gradient directions. Finally, the local image gradients are evaluated at the selected scale in the region around each keypoint [19]. In the identification stage, the Euclidean distance can be employed to determine the identity of the query image. A smaller Euclidean distance means a higher similarity between the query image and the training image.

## III. THE PROPOSED FRAMEWORK

### A. Similarity Between the Left and Right Palmprints

In this subsection the illustration of the correlation between the left and right palmprints is presented. Fig. 2 shows palmprint images of four subjects. Fig. 2 (a)-(d) show four left palmprint images of these four subjects. Fig. 2 (e)-(h) show four right palmprint images of the same four subjects. Images in Fig. 2 (i)-(l) are the four reverse palmprint images of those shown in Fig. 2 (e)-(h). It can be seen that the left palmprint image and the reverse right palmprint image of the same subject are somewhat similar.

Fig. 3 (a)-(d) depict the principal lines images of the left palmprint shown in Fig. 2 (a)-(d). Fig. 3 (e)-(h) are the reverse right palmprint principal lines images corresponding to Fig. 2 (i)-(l). Fig. 3 (i)-(l) show the principle lines matching images of Fig. 3 (a)-(d) and Fig. 3 (e)-(h), respectively. Fig. 3 (m)-(p) are matching images between the left and reverse right palmprint principal lines images from different subjects. The four matching images of Fig. 3 (m)-(p)

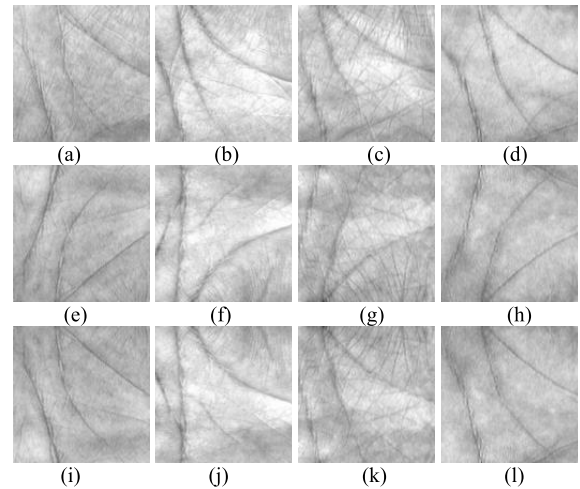


Fig. 2. Palmprint images of four subjects. (a)-(d) are four left palmprint images; (e)-(h) are four right palmprint corresponding to (a)-(d); (i)-(l) are the reverse right palmprint images of (e)-(h).

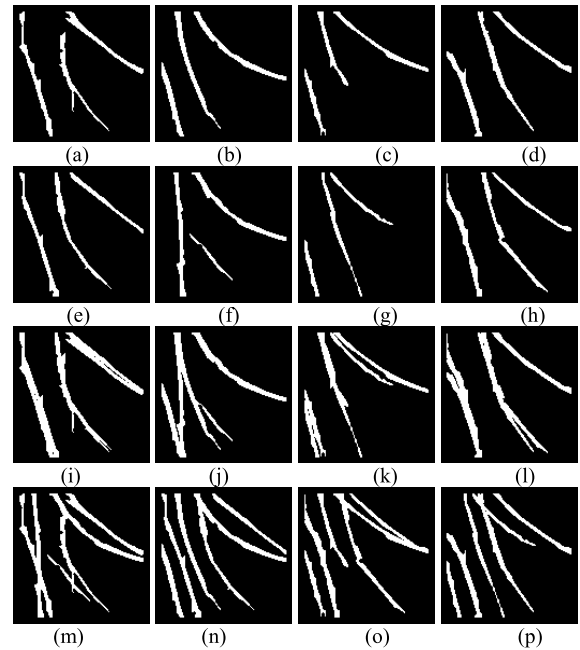


Fig. 3. Principal lines images. (a)-(d) are four left palmprint principal lines images, (e)-(h) are four reverse right palmprint principal lines image, (i)-(l) are principal lines matching images of the same people, and (m)-(p) are principal lines matching images from different people.

are: (a) and (f) principal lines matching image, (b) and (e) principal lines matching image, (c) and (h) principal lines matching image, and (d) and (g) principal lines matching image, respectively.

Fig. 3 (i)-(l) clearly show that principal lines of the left and reverse right palmprint from the same subject have very similar shape and position. However, principal lines of the left and right palmprint from different individuals have very different shape and position, as shown in Fig. 3 (m)-(p). This demonstrates that the principal lines of the left palmprint and reverse right palmprint can also be used for palmprint verification/identification.

## B. Procedure of the Proposed Framework

This subsection describes the main steps of the proposed framework. The framework first works for the left palmprint images and uses a palmprint identification method to calculate the scores of the test sample with respect to each class. Then it applies the palmprint identification method to the right palmprint images to calculate the score of the test sample with respect to each class. After the crossing matching score of the left palmprint image for testing with respect to the reverse right palmprint images of each class is obtained, the proposed framework performs matching score level fusion to integrate these three scores to obtain the identification result. The method is presented in detail below.

We suppose that there are  $C$  subjects, each of which has  $m$  available left palmprint images and  $m$  available right palmprint images for training. Let  $X_i^k$  and  $Y_i^k$  denote the  $i$ th left palmprint image and  $i$ th right palmprint image of the  $k$ th subject respectively, where  $i = 1, \dots, m$  and  $k = 1, \dots, C$ . Let  $Z_1$  and  $Z_2$  stand for a left palmprint image and the corresponding right palmprint image of the subject to be identified.  $Z_1$  and  $Z_2$  are the so-called test samples.

*Step 1:* Generate the reverse images  $\tilde{Y}_i^k$  of the right palmprint images  $Y_i^k$ . Both  $Y_i^k$  and  $\tilde{Y}_i^k$  will be used as training samples.  $\tilde{Y}_i^k$  is obtained by:  $\tilde{Y}_i^k(l, c) = Y_i^k(L_Y - l + 1, c)$ , ( $l = 1 \dots L_Y$ ,  $c = 1 \dots C_Y$ ), where  $L_Y$  and  $C_Y$  are the row number and column number of  $Y_i^k$  respectively.

*Step 2:* Use  $Z_1$ ,  $X_i^k$  s and a palmprint identification method, such as the method introduced in Section II, to calculate the score of  $Z_1$  with respect to each class. The score of  $Z_1$  with respect to the  $i$ th class is denoted by  $s_i$ .

*Step 3:* Use  $Z_2$ ,  $Y_i^k$  s and the palmprint identification method used in Step 2 to calculate the score of  $Z_2$  with respect to each class. The score of  $Z_2$  with respect to the  $i$ th class is denoted by  $t_i$ .

*Step 4:*  $\tilde{Y}_j^k$  ( $j = 1, \dots, m'$ ,  $m' \leq m$ ), which have the property of  $\text{Sim\_score}(\tilde{Y}_j^k, X^k) \geq \text{match\_threshold}$ , are selected from  $\tilde{Y}^k$  as additional training samples, where  $\text{match\_threshold}$  is a threshold.  $\text{Sim\_score}(\tilde{Y}_j^k, X^k)$  is defined as:

$$\text{Sim\_score}(Y, X^k) = \frac{\sum_{t=1}^T (S(\hat{Y}_t, X^k))}{T}, \quad (8)$$

and

$$S(\hat{Y}_t, X^k) = \max(\text{Score}(\hat{Y}_t, \hat{X}_i^k)), \quad i = \{1 \dots m\}, \quad (9)$$

where  $Y$  is a palmprint image.  $X^k$  are a set of palmprint images from the  $k$ th subject and  $X_i^k$  is one image from  $X^k$ .  $\hat{X}_i^k$  and  $\hat{Y}$  are the principal line images of  $X_i^k$  and  $Y$ , respectively.  $T$  is the number of principal lines of the palmprint and  $t$  represent the  $t$ th principal line.  $\text{Score}(Y, X)$  is calculated as formula (1) and the  $\text{Score}(Y, X)$  is set to 0 when it is smaller than  $\text{sim\_threshold}$ , which is empirically set to 0.15.

*Step 5:* Treat  $\tilde{Y}_j^k$  s obtained in Step 4 as the training samples of  $Z_1$ . Use the palmprint identification method used in Step 2 to calculate the score of  $Z_1$  with respect to each class.

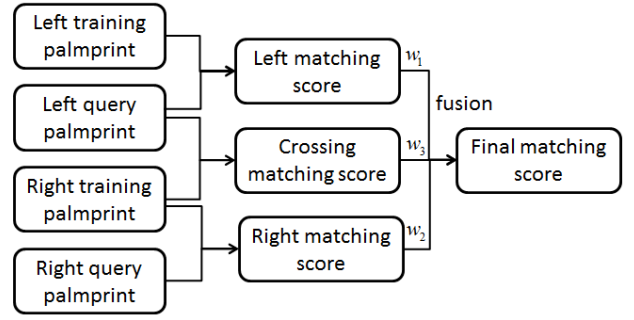


Fig. 4. Fusion at the matching score level of the proposed framework.

The score of the test sample with respect to  $\tilde{Y}_j^k$  s of the  $i$ th class is denoted as  $g_i$ .

*Step 6:* The weighted fusion scheme  $f_i = w_1 s_i + w_2 t_i + w_3 g_i$ , where  $0 \leq w_1, w_2 \leq 1$  and  $w_3 = 1 - w_1 - w_2$ , is used to calculate the score of  $Z_1$  with respect to the  $i$ th class. If  $q = \arg \min_i f_i$ , then the test sample is recognized as the  $q$ th subject.

## C. Matching Score Level Fusion

In the proposed framework, the final decision making is based on three kinds of information: the left palmprint, the right palmprint and the correlation between the left and right palmprint. As we know, fusion in multimodal biometric systems can be performed at four levels. In the image (sensor) level fusion, different sensors are usually required to capture the image of the same biometric. Fusion at decision level is too rigid since only abstract identity labels decided by different matchers are available, which contain very limited information about the data to be fused. Fusion at feature level involves the use of the feature set by concatenating several feature vectors to form a large 1D vector. The integration of features at the earlier stage can convey much richer information than other fusion strategies. So feature level fusion is supposed to provide a better identification accuracy than fusion at other levels. However, fusion at the feature level is quite difficult to implement because of the incompatibility between multiple kinds of data. Moreover, concatenating different feature vectors also lead to a high computational cost. The advantages of the scorelevel fusion have been concluded in [21], [22], and [39] and the weight-sum scorelevel fusion strategy is effective for component classifier combination to improve the performance of biometric identification. The strength of individual matchers can be highlighted by assigning a weight to each matching score. Consequently, the weight-sum matching score level fusion is preferable due to the ease in combining three kinds of matching scores of the proposed method.

Fig. 4 shows the basic fusion procedure of the proposed method at the matching score level. The final matching score is generated from three kinds of matching scores. The first and second matching scores are obtained from the left and right palmprint, respectively. The third kind of score is calculated based on the crossing matching between the left and right palmprint.  $w_i$  ( $i = 1, 2, 3$ ), which denotes the weight assigned to the  $i$ th matcher, can be adjusted and viewed as the importance of the corresponding matchers.

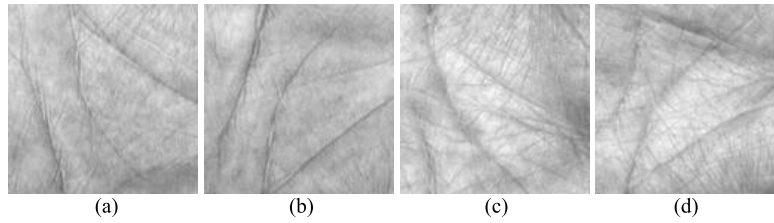


Fig. 5. (a)-(d) are two pairs of the left and right palmprint images of two subjects from PolyU database.

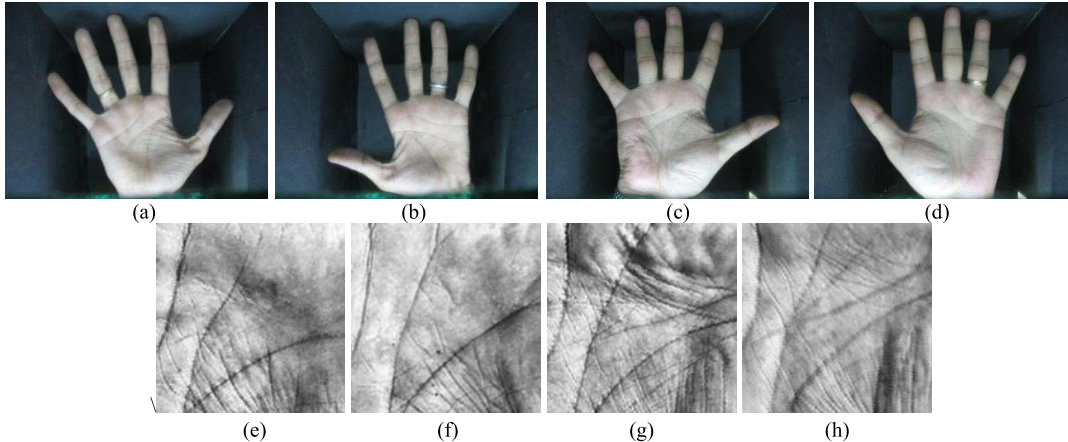


Fig. 6. (a)-(d) are two pairs of the left and right hand images of two subjects from IITD database. (e)-(h) are the corresponding ROI images extracted from (a) and (d).

Differing from the conventional matching score level fusion, the proposed method introduces the crossing matching score to the fusion strategy. When  $w_3 = 0$ , the proposed method is equivalent to the conventional score level fusion. Therefore, the performance of the proposed method will at least be as good as or even better than conventional methods by suitably tuning the weight coefficients.

#### IV. EXPERIMENTAL RESULTS

More than 7,000 different images from both the contact-based and the contactless palmprint databases are employed to evaluate the effectiveness of the proposed method. Typical state-of-the-art palmprint identification methods, such as the RLOC method, the competitive code method, the ordinal code method, the BOCV method, and the SMCC method [7], are adopted to evaluate the performance of the proposed framework. Moreover, several recent developed contactless based methods, such as the SIFT methods [19] and the OLOF+SIFT method [20], are also used to test the proposed framework. For the sake of completeness, we compare the performance of our method with that of the conventional fusion based methods.

##### A. Palmprint Databases

The PolyU palmprint database (version 2) [40] contains 7,752 palmprint images captured from a total of 386 palms of 193 individuals. The samples of each individual were collected in two sessions, where the average interval between the first and second sessions was around two months. In each session, each individual was asked to provide about 10 images of each palm. We notice that some individual provide few images. For example, only one image of the 150th individual was captured in the second session. To facilitate the

evaluation of the performance of our framework, we set up a subset from the whole database by choosing 3,740 images of 187 individual, where each individual provide 10 right palmprint images and 10 left palmprint images, to carry out the following experiments. Fig. 5 shows some palmprint samples on the PolyU database.

The public IITD palmprint database [41] is a contactless palmprint database. Images in IITD database were captured in the indoor environment, which acquired contactless hand images with severe variations in pose, projection, rotation and translation. The main problem of contactless databases lies in the significant intra-class variations resulting from the absence of any contact or guiding surface to restrict such variations [20]. The IITD database consists of 3,290 hand images from 235 subjects. Seven hand images were captured from each of the left and right hand for each individual in every session. In addition to the original hand images, the Region Of Interest (ROI) of palmprint images are also available in the database. Fig. 6 shows some typical hand images and the corresponding ROI palmprint images in the IITD palmprint database. Compared to the palmprint images in the PolyU database, the images in the IITD database are more close to the real-applications.

##### B. Matching Results Between the Left and Right Palmprint

To obtain the correlation between the left and right palmprint in both the PolyU and the IITD databases, each left palmprint is matched with every right palmprint of each subject and the principal line matching score is calculated for the left palmprint and this subject. A match is counted as a genuine matching if the left palmprint is from the class; if otherwise, the match is counted as an imposter matching.

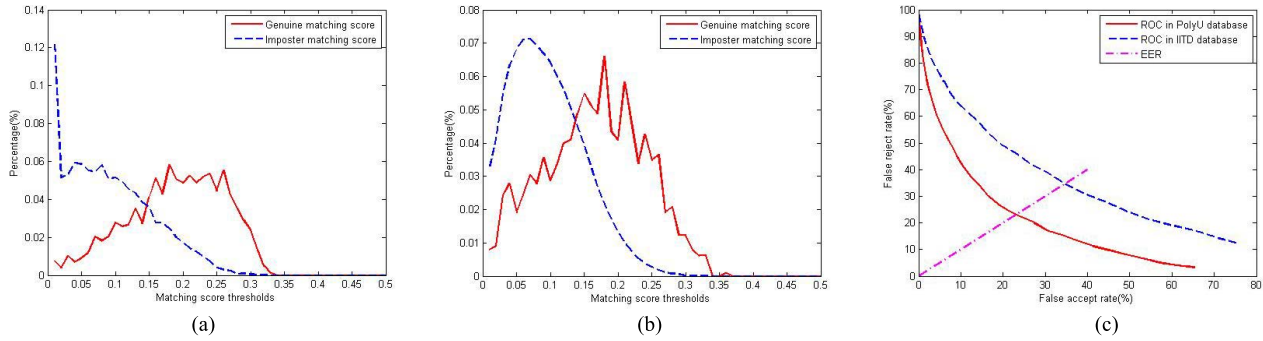


Fig. 7. (a) and (b) are matching score distributions of the PolyU and IITD databases, respectively. (c) is ROC curves of the PolyU and IITD databases.

The PolyU palmprint subethas 1,870 left palmprint images and 1,870 right palmprints from 187 individuals. Therefore there are 1,870 (1870\*1) genuine matches and 347,820 (1870\*186) imposter matches in total. In the IITD palmprint database, there are 1,645 left palmprint images and 1,645 right palmprints from 235 different subjects. So in the IITD database the total number of genuine matching and imposter matching are 1,645 (1645\*1) and 384,930 (1645\*234), respectively. The training sample number of each class in both experiments are set as 3 and 2, respectively. Fig. 7 (a)-(b) show the matching results of both databases. The False Accept Rate (FAR), False Reject Rate (FRR) and Equal Error Rate (EER) (the point where FAR is equal to FRR) [1] are adopted to evaluate the similarity between the left and right palmprints. The Receiver Operating Characteristic (ROC) curve, which is a graph of FRR against FAR for all possible thresholds, is introduced to describe the performance of the proposed method. The ROC curves of both the PolyU and IITD databases are plotted in Fig. 7 (c).

Fig. 7 (a)-(b) show that the genuine matching generally have larger principal lines matching scores than those of the imposter matching. The distribution of the genuine matching and imposter matching are separable and the genuine class and the imposter class can be roughly discriminated by using a linear classifier. The EERs of two databases are 24.22% and 35.82%, respectively. One can observe that the EER obtained using the IITD database is much larger than that obtained using the PolyU database. The main reason is that palmprint images in IITD database have serious variations in rotation and translation. The experimental results still illustrate that the left palmprint and right palmprint of the same people generally have higher similarity than those from different subjects.

C. Experimental Results on PolyU Palmprint Database

In identification experiments, different kinds of palmprint recognition methods are applied in the framework, including the line based method [10], coding based methods, subspace based methods, and representation based methods.

In the experiments, *match\_threshold* is empirically set to 0.2. The conventional fusion scheme only fuses the left palmprint and right palmprint features, but does not integrate the crossing similarity between the left and right palmprint.

TABLE I  
RESULTS OF THE RLOC WITH *m* AS 2 AND THE COMPETITIVE CODE METHOD WITH *m* AS 1

RLOC				Competitive code method			
<i>w</i> <sub>1</sub>	<i>w</i> <sub>2</sub>	<i>w</i> <sub>3</sub>	error rate	<i>w</i> <sub>1</sub>	<i>w</i> <sub>2</sub>	<i>w</i> <sub>3</sub>	error rate
0.5	0.5	0	5.21%	0.4	0.6	0	0.48%
0.6	0.4	0	5.95%	0.5	0.5	0	0.48%
0.55	0.45	0	5.82%	0.6	0.4	0	0.83%
0.45	0.5	0.05	5.15%	0.45	0.5	0.05	0.42%
0.45	0.45	0.1	5.01%	0.3	0.6	0.1	0.30%

TABLE II  
RESULTS OF THE ORDINAL CODE METHOD WITH *m* AS 1 AND THE FUSION CODE METHOD WITH *m* AS 1

Ordinal code method				Fusion code method			
<i>w</i> <sub>1</sub>	<i>w</i> <sub>2</sub>	<i>w</i> <sub>3</sub>	error rate	<i>w</i> <sub>1</sub>	<i>w</i> <sub>2</sub>	<i>w</i> <sub>3</sub>	error rate
0.4	0.6	0	0.83%	0.5	0.5	0	0.59%
0.35	0.65	0	0.89%	0.3	0.7	0	0.59%
0.55	0.45	0	0.89%	0.45	0.55	0	0.59%
0.35	0.6	0.05	0.77%	0.4	0.55	0.05	0.53%
0.4	0.55	0.05	0.83%	0.3	0.65	0.05	0.53%

TABLE III  
RESULTS OF THE PALMCODE METHOD WITH *m* AS 1 AND THE BOCV METHOD WITH *m* AS 1

Palmcode				BOCV			
<i>w</i> <sub>1</sub>	<i>w</i> <sub>2</sub>	<i>w</i> <sub>3</sub>	error rate	<i>w</i> <sub>1</sub>	<i>w</i> <sub>2</sub>	<i>w</i> <sub>3</sub>	error rate
0.4	0.6	0	0.77%	0.5	0.5	0	0.71%
0.6	0.4	0	0.65%	0.4	0.6	0	0.59%
0.55	0.45	0	0.42%	0.35	0.65	0	0.53%
0.45	0.45	0.1	0.36%	0.3	0.65	0.05	0.48%
0.5	0.45	0.05	0.36%	0.35	0.6	0.05	0.48%

So the conventional fusion scheme is a special case of the proposed framework with *w*<sub>3</sub> = 0. Three weight coefficients are assigned to three scores. The weight coefficients *w*<sub>1</sub>, *w*<sub>2</sub> and *w*<sub>3</sub> are tuned in step of 0.05. The left palmprint matching scores and right palmprint matching scores should have larger weights than the crossing matching score between the left palmprint and reverse right palmprint.

TABLE IV  
RESULTS OF THE 2DPCA BASED METHOD WITH  $m$  AS 2 AND  
THE 2DLDA BASED METHOD WITH  $m$  AS 3

2DPCA				2DLDA			
$w_1$	$w_2$	$w_3$	error rate	$w_1$	$w_2$	$w_3$	error rate
0.5	0.5	0	4.81%	0.55	0.45	0	0.46%
0.6	0.4	0	4.75%	0.4	0.6	0	0.38%
0.35	0.65	0	4.88%	0.6	0.4	0	0.53%
0.5	0.4	0.05	4.55%	0.4	0.5	0.1	0.31%
0.45	0.45	0.1	4.61%	0.5	0.45	0.05	0.31%

TABLE V  
RESULTS OF THE PCA BASED METHOD WITH  $m$  AS 4 AND  
THE LDA BASED METHOD WITH  $m$  AS 2

PCA				LDA			
$w_1$	$w_2$	$w_3$	error rate	$w_1$	$w_2$	$w_3$	error rate
0.45	0.55	0	0.27%	0.5	0.5	0	0.13%
0.6	0.4	0	0.27%	0.4	0.6	0	0.13%
0.35	0.65	0	0.36%	0.6	0.4	0	0.13%
0.55	0.4	0.05	0.18%	0.4	0.4	0.2	0.07%
0.45	0.45	0.1	0.18%	0.5	0.4	0.1	0.07%

TABLE VI  
RESULTS OF THE TPTSSR METHOD WITH  $m$  AS 1 AND  
THE CRC BASED METHOD WITH  $m$  AS 1

TPTSSR				CRC			
$w_1$	$w_2$	$w_3$	error rate	$w_1$	$w_2$	$w_3$	error rate
0.5	0.5	0	0.83%	0.5	0.5	0	0.83%
0.6	0.4	0	1.43%	0.55	0.45	0	0.77%
0.3	0.7	0	1.13%	0.45	0.55	0	1.07%
0.4	0.5	0.1	0.65%	0.5	0.45	0.05	0.65%
0.4	0.55	0.05	0.71%	0.4	0.5	0.1	0.65%

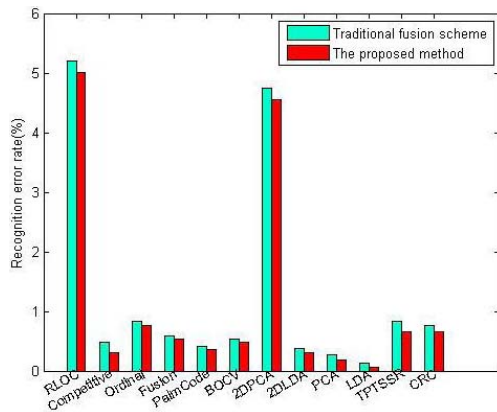


Fig. 8. The comparative results between the proposed method and the conventional fusion method on the PolyU database.

It is impossible to exhaustively verify all possible weight coefficients to find the optimal coefficients. Due to the limit of space, only a set of representative weight coefficients that minimize the final identification error rate of our framework

TABLE VII  
RESULTS OF ORDINAL CODE METHOD WITH  $m$  AS 2 AND  
THE SIFT BASED METHOD WITH  $m$  AS 2

Ordinal code method				SIFT			
$w_1$	$w_2$	$w_3$	error rate	$w_1$	$w_2$	$w_3$	error rate
0.5	0.5	0	1.16%	0.5	0.5	0	5.94%
0.4	0.6	0	1.74%	0.4	0.6	0	5.94%
0.6	0.4	0	1.30%	0.6	0.4	0	6.09%
0.4	0.	0.2	1.01%	0.4	0.5	0.1	5.36%
0.5	0.4	0.1	1.16%	0.45	0.5	0.05	5.51%

and conventional fusion methods are reported. Empirically, the score that has the lower identification error rate usually has a larger weight coefficient. In addition, the optimal weight coefficients vary with the methods, since each method adopted in the proposed framework utilizes different palmprint feature extraction algorithm.

The first  $m$  left and  $m$  right palmprint are selected as the training samples to calculate the left matching score  $s_i$  and the right matching score  $t_i$ , respectively. The rest of the left and right palmprints are used as test samples.  $m$  reverse right palmprints are also selected as the training samples to calculate the crossing matching score  $g_i$  based on the rule of the proposed framework. Table I-VI list the identification error rate of the proposed framework using different palmprint identification methods.

The experimental results of the PolyU database show that the identification error rate of the proposed method is about 0.06% to 0.2% lower than that of conventional fusion methods. The comparison between the best identification results of the proposed method and conventional fusion scheme are depicted as Fig. 8, which shows that the framework using different methods outperform the conventional fusion schemes.

#### D. Experimental Results on IITD Palmprint Database

Experiments are also conducted on the IITD contactless palmprint database. For the space limited, not all methods employed in the PolyU database but several promising contactless palmprint identification methods, including coding based methods, the SIFT based method, the OLOF+SIFT method and the SMCC method, are adopted to carry out the experiments. In addition, LDA and CRC based methods are also tested by the database. Large scale translation will cause serious false position problem in the IITD database. To reduce the effect of the image translation between the test image and the training image, the test image will be vertically and horizontally translated with one to three pixels, and the best matching result obtained from the translated matching is recorded as the final matching result. The experimental results are listed in Table VII-X. The corresponding comparison between the best identification accuracies of the proposed method and conventional fusion schemes are plotted as Fig. 9.

Both Fig. 8 and 9 clearly show that the palmprint identification accuracy of the proposed framework is higher than that of the direct fusion of the left and right palmprint for both

TABLE VIII  
RESULTS OF OLOF+SIFT WITH  $m$  AS 2 AND  
THE BOCV METHOD  $m$  AS 2

OLOF+SIFT				BOCV			
$w_1$	$w_2$	$w_3$	error rate	$w_1$	$w_2$	$w_3$	error rate
0.5	0.5	0	0.72%	0.5	0.5	0	2.03%
0.4	0.6	0	0.58%	0.45	0.55	0	2.17%
0.35	0.65	0	0.58%	0.6	0.4	0	2.46%
0.4	0.5	0.1	0.43%	0.45	0.45	0.1	2.03%
0.3	0.6	0.1	0.58%	0.5	0.45	0.05	1.74%

TABLE IX  
RESULTS OF PALMCODE METHOD WITH  $m$  AS 2 AND  
THE SMCC METHOD WITH  $m$  AS 1

Palmcode				SMCC			
$w_1$	$w_2$	$w_3$	error rate	$w_1$	$w_2$	$w_3$	error rate
0.5	0.5	0	3.04%	0.4	0.6	0	0.54%
0.4	0.6	0	3.77%	0.5	0.4	0	0.54%
0.6	0.4	0	3.48%	0.45	0.55	0	0.54%
0.45	0.45	0.1	2.90%	0.4	0.	0.2	0.43%
0.5	0.4	0.1	2.90%	0.45	0.45	0.1	0.43%

TABLE X  
RESULTS OF LDA METHOD WITH  $m$  AS 2 AND  
THE CRC METHOD WITH  $m$  AS 1

LDA				CRC			
$w_1$	$w_2$	$w_3$	error rate	$w_1$	$w_2$	$w_3$	error rate
0.5	0.5	0	10.29%	0.5	0.5	0	12.90%
0.4	0.6	0	10.29%	0.4	0.6	0	14.06%
0.35	0.65	0	10.43%	0.6	0.4	0	13.33%
0.45	0.5	0.05	10.14%	0.4	0.5	0.1	12.75%
0.4	0.55	0.05	10.29%	0.4	0.4	0.2	12.75%

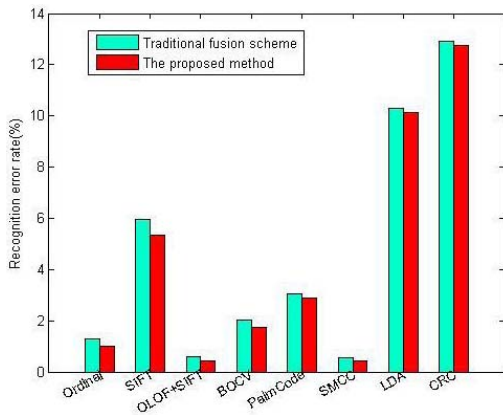


Fig. 9. The comparative results between the proposed method and the conventional fusion method in the IITD database.

the PolyU database and the IITD contactless database. As a result, we infer that the use of the similarity between the left and right palmprint is effective for improving the performance of palmprint identification.

TABLE XI  
COMPUTATIONAL TIME OF IDENTIFICATION

Methods used in individual matcher	Conventional strategy	The proposed method
RLOC	1.16s	1.74s
Competitive code	0.26s	0.39s
Palmcode	0.54s	0.80s
LDA	19.70ms	29.73ms
TPTTSR	41.91ms	62.88ms
SIFT+OLOF	15.62s	24.14s
SMCC	10.94s	16.06s

It seems that the crossing matching score can also be calculated based on the similarity between the right query and left training palmprint. We also conduct experiments to fuse both crossing matching scores to perform palmprint identification. However, as the use of the two crossing matching scores does not lead to more accuracy improvement, we exploit only one of them in the proposed method.

### E. Computational Complexity

In the proposed method, since the processing of the reverse right training palmprint can be performed before palmprint identification, the main computational cost of the proposed method largely relies on the individual palmprint identification method. Compared to the conventional fusion strategy that only fuses two individual matchers, the proposed method consists of three individual matches. As a result, the proposed method needs to perform one more identification than the conventional strategy. Thus, the identification time of the proposed method may be about 1.5 times of that of conventional fusion strategy.

To evaluate the computational cost of the proposed method, algorithms adopted in the proposed method are implemented by using MATLAB 7.10.0 on a PC with double-core Intel(R) i5-3470 (3.2GHz), RAM 8.00GB, and Windows 7.0 operating system. The time taken for the processing the reverse right training palmprint for each class is about 4.24s and 2.91s on both databases. Some representative average identification time of the proposed method and conventional fusion strategy are shown in Table. XI.

## V. CONCLUSIONS

This study shows that the left and right palmprint images of the same subject are somewhat similar. The use of this kind of similarity for the performance improvement of palmprint identification has been explored in this paper. The proposed method carefully takes the nature of the left and right palmprint images into account, and designs an algorithm to evaluate the similarity between them. Moreover, by employing this similarity, the proposed weighted fusion scheme uses a method to integrate the three kinds of scores generated from the left and right palmprint images. Extensive experiments demonstrate that the proposed framework obtains very high accuracy and the use of the similarity score between the left

and right palmprint leads to important improvement in the accuracy. This work also seems to be helpful in motivating people to explore potential relation between the traits of other bimodal biometrics issues.

#### ACKNOWLEDGMENT

Thanks to Dr. Edward C. Mignot, Shandong University, for linguistic advice.

#### REFERENCES

- [1] A. W. K. Kong, D. Zhang, and M. S. Kamel, "A survey of palmprint recognition," *Pattern Recognit.*, vol. 42, no. 7, pp. 1408–1418, Jul. 2009.
- [2] D. Zhang, W. Zuo, and F. Yue, "A comparative study of palmprint recognition algorithms," *ACM Comput. Surv.*, vol. 44, no. 1, pp. 1–37, Jan. 2012.
- [3] D. Zhang, F. Song, Y. Xu, and Z. Lang, "Advanced pattern recognition technologies with applications to biometrics," *Med. Inf. Sci. Ref.*, Jan. 2009, pp. 1–384.
- [4] R. Chu, S. Liao, Y. Han, Z. Sun, S. Z. Li, and T. Tan, "Fusion of face and palmprint for personal identification based on ordinal features," in *Proc. IEEE Conf. Comput. Vis. Pattern Recognit. (CVPR)*, Jun. 2007, pp. 1–2.
- [5] D. Zhang, W.-K. Kong, J. You, and M. Wong, "Online palmprint identification," *IEEE Trans. Pattern Anal. Mach. Intell.*, vol. 25, no. 9, pp. 1041–1050, Sep. 2003.
- [6] A.-W. K. Kong and D. Zhang, "Competitive coding scheme for palmprint verification," in *Proc. 17th Int. Conf. Pattern Recognit.*, vol. 1, Aug. 2004, pp. 520–523.
- [7] W. Zuo, Z. Lin, Z. Guo, and D. Zhang, "The multiscale competitive code via sparse representation for palmprint verification," in *Proc. IEEE Conf. Comput. Vis. Pattern Recognit. (CVPR)*, Jun. 2010, pp. 2265–2272.
- [8] Z. Sun, T. Tan, Y. Wang, and S. Z. Li, "Ordinal palmprint representation for personal identification [representation read representation]," in *Proc. IEEE Conf. Comput. Vis. Pattern Recognit.*, vol. 1, Jun. 2005, pp. 279–284.
- [9] A. Kong, D. Zhang, and M. Kamel, "Palmprint identification using feature-level fusion," *Pattern Recognit.*, vol. 39, no. 3, pp. 478–487, Mar. 2006.
- [10] D. S. Huang, W. Jia, and D. Zhang, "Palmprint verification based on principal lines," *Pattern Recognit.*, vol. 41, no. 4, pp. 1316–1328, Apr. 2008.
- [11] S. Ribaric and I. Fratric, "A biometric identification system based on eigenpalm and eigenfinger features," *IEEE Trans. Pattern Anal. Mach. Intell.*, vol. 27, no. 11, pp. 1698–1709, Nov. 2005.
- [12] K.-H. Cheung, A. Kong, D. Zhang, M. Kamel, and J. You, "Does EigenPalm work? A system and evaluation perspective," in *Proc. IEEE 18th Int. Conf. Pattern Recognit.*, vol. 4, 2006, pp. 445–448.
- [13] J. Gui, W. Jia, L. Zhu, S.-L. Wang, and D.-S. Huang, "Locality preserving discriminant projections for face and palmprint recognition," *Neurocomputing*, vol. 73, nos. 13–15, pp. 2696–2707, Aug. 2010.
- [14] P. N. Belhumeur, J. P. Hespanha, and D. Kriegman, "Eigenfaces vs. fisherfaces: Recognition using class specific linear projection," *IEEE Trans. Pattern Anal. Mach. Intell.*, vol. 19, no. 7, pp. 711–720, Jul. 1997.
- [15] H. Sang, W. Yuan, and Z. Zhang, "Research of palmprint recognition based on 2DPCA," in *Advances in Neural Networks ISNN* (Lecture Notes in Computer Science). Berlin, Germany: Springer-Verlag, 2009, pp. 831–838.
- [16] F. Du, P. Yu, H. Li, and L. Zhu, "Palmprint recognition using Gabor feature-based bidirectional 2DLDA," *Commun. Comput. Inf. Sci.*, vol. 159, no. 5, pp. 230–235, 2011.
- [17] D. Hu, G. Feng, and Z. Zhou, "Two-dimensional locality preserving projections (2DLPP) with its application to palmprint recognition," *Pattern Recognit.*, vol. 40, no. 1, pp. 339–342, Jan. 2007.
- [18] Y. Xu, Z. Fan, M. Qiu, D. Zhang, and J.-Y. Yang, "A sparse representation method of bimodal biometrics and palmprint recognition experiments," *Neurocomputing*, vol. 103, pp. 164–171, Mar. 2013.
- [19] D. G. Lowe, "Distinctive image features from scale-invariant keypoints," *Int. J. Comput. Vis.*, vol. 60, no. 2, pp. 91–110, Nov. 2004.
- [20] A. Morales, M. A. Ferrer, and A. Kumar, "Towards contactless palmprint authentication," *IET Comput. Vis.*, vol. 5, no. 6, pp. 407–416, Nov. 2011.
- [21] A. K. Jain, A. Ross, and S. Prabhakar, "An introduction to biometric recognition," *IEEE Trans. Circuits Syst. Video Technol.*, vol. 14, no. 1, pp. 4–20, Jan. 2004.
- [22] Y. Xu, Q. Zhu, D. Zhang, and J. Y. Yang, "Combine crossing matching scores with conventional matching scores for bimodal biometrics and face and palmprint recognition experiments," *Neurocomputing*, vol. 74, no. 18, pp. 3946–3952, Nov. 2011.
- [23] S. Tulyakov and V. Govindaraju, "Use of identification trial statistics for the combination of biometric matchers," *IEEE Trans. Inf. Forensics Security*, vol. 3, no. 4, pp. 719–733, Dec. 2008.
- [24] D. Zhang, Z. Guo, G. Lu, D. Zhang, and W. Zuo, "An online system of multispectral palmprint verification," *IEEE Trans. Instrum. Meas.*, vol. 59, no. 2, pp. 480–490, Feb. 2010.
- [25] Y. Hao, Z. Sun, and T. Tan, "Comparative studies on multispectral palmimage fusion for biometrics," in *Proc. 8th Asian Conf. Comput. Vis.*, Nov. 2007, pp. 12–21.
- [26] D. Han, Z. Guo, and D. Zhang, "Multispectral palmprint recognition using wavelet-based image fusion," in *Proc. IEEE 9th Int. Conf. Signal Process.*, Oct. 2008, pp. 2074–2077.
- [27] A. Kumar, D. C. M. Wong, and H. C. Shen, "Personal verification using palmprint and hand geometry biometric," in *Audio-and Video-Based Biometric Person Authentication* (Lecture Notes in Computer Science). Berlin, Germany: Springer-Verlag, 2003, pp. 668–678.
- [28] G. Feng, K. Dong, and D. Hu, "When faces are combined with palmprints: A novel biometric fusion strategy," in *Biometric Authentication* (Lecture Notes in Computer Science). Berlin, Germany: Springer-Verlag, 2004, pp. 701–707.
- [29] Y.-F. Yao, X.-Y. Jing, and H.-S. Wong, "Face and palmprint feature level fusion for single sample biometrics recognition," *Neurocomputing*, vol. 70, nos. 7–9, pp. 1582–1586, Mar. 2007.
- [30] D. Zhang, Z. Guo, G. Liu, L. Zhang, Y. Liu, and W. Zuo, "Online joint palmprint and palmvein verification," *Expert Syst. Appl.*, vol. 38, no. 3, pp. 2621–2631, Mar. 2011.
- [31] J. Dai and J. Zhou, "Multifeature-based high-resolution palmprint recognition," *IEEE Trans. Pattern Anal. Mach. Intell.*, vol. 33, no. 5, pp. 945–957, May 2011.
- [32] A. Kumar and D. Zhang, "Personal authentication using multiple palmprint representation," *Pattern Recognit.*, vol. 38, no. 10, pp. 1695–1704, 2005.
- [33] W. Jia, D. Huang, and D. Zhang, "Palmprint verification based on robust line orientation code," *Pattern Recognit.*, vol. 41, no. 5, pp. 1504–1513, May 2008.
- [34] Z. Guo, D. Zhang, L. Zhang, and W. Zuo, "Palmprint verification using binary orientation co-occurrence vector," *Pattern Recognit. Lett.*, vol. 30, no. 13, pp. 1219–1227, Oct. 2009.
- [35] Y. Xu, D. Zhang, J. Yang, and J.-Y. Yang, "A two-phase test sample sparse representation method for use with face recognition," *IEEE Trans. Circuits Syst. Video Technol.*, vol. 21, no. 9, pp. 1255–1262, Sep. 2011.
- [36] L. Zhang, M. Yang, and X. Feng, "Sparse representation or collaborative representation: Which helps face recognition," in *Proc. IEEE Int. Conf. Comput. Vis.*, 2011, pp. 471–478.
- [37] Z. Guo, G. Wu, Q. Chen, and W. Liu, "Palmprint recognition by a two-phase test sample sparse representation," in *Proc. Int. Conf. Hand-Based Biometrics (ICHB)*, Nov. 2011, pp. 1–4.
- [38] X. Wu, Q. Zhao, and W. Bu, "A SIFT-based contactless palmprint verification approach using iterative RANSAC and local palmprint descriptors," *Pattern Recognition*, vol. 47, no. 10, pp. 3314–3326, Oct. 2014.
- [39] A. K. Jain and J. Feng, "Latent palmprint matching," *IEEE Trans. Pattern Anal. Mach. Intell.*, vol. 31, no. 6, pp. 1032–1047, Jun. 2009.
- [40] *PolyU Palmprint Image Database Version 2.0*. [Online]. Available: <http://www.comp.polyu.edu.hk/~biometrics/>, accessed 2003.
- [41] *IITD Touchless Palmprint Database, Version 1.0*. [Online]. Available: [http://www4.comp.polyu.edu.hk/~csajaykr/IITD/Database\\_Palm.htm](http://www4.comp.polyu.edu.hk/~csajaykr/IITD/Database_Palm.htm), accessed 2008.



**Yong Xu** (M'06) received the B.S. and M.S. degrees, in 1994 and 1997, respectively, and the Ph.D. degree in pattern recognition and intelligence system from the Nanjing University of Science and Technology, Nanjing, China, in 2005. He is currently with the Research Center of Biocomputing, Harbin Institute of Technology Shenzhen Graduate School, Shenzhen, China. His current research interests include pattern recognition, biometrics, bioinformatics, machine learning, image processing, and video analysis.



**Lunke Fei** received the B.S. and M.S. degrees in computer science and technology from East China Jiaotong University, Nanchang, China, in 2004 and 2007, respectively. He is currently pursuing the Ph.D. degree in computer science and technology with the Harbin Institute of Technology Shenzhen Graduate School, Shenzhen, China. His current research interests include pattern recognition and biometrics.



**David Zhang** (F'08) received the degree in computer science from Peking University, Beijing, China, and the M.Sc. degree in computer science and Ph.D. degree from the Harbin Institute of Technology (HIT), Harbin, China, in 1982 and 1985, respectively. From 1986 to 1988, he was a Post-Doctoral Fellow with Tsinghua University, Beijing, and an Associate Professor with Academia Sinica, Beijing. In 1994, he received the second Ph.D. degree in electrical and computer engineering from the University of Waterloo, Ontario, ON, Canada.

He is currently the Head of the Department of Computing, and a Chair Professor with the Hong Kong Polytechnic University, Hong Kong, where he is the Founding Director of the Biometrics Technology Centre supported by the Hong Kong Government in 1998. He serves as a Visiting Chair Professor with Tsinghua University and an Adjunct Professor with Peking University, Shanghai Jiao Tong University, Shanghai, China, HIT, and the University of Waterloo. He is the Founder and an Editor-In-Chief of the *International Journal of Image and Graphics*, a Book Editor of the *Springer International Series on Biometrics*, an Organizer of the *International Conference on Biometrics Authentication*, an Associate Editor of more than 10 international journals, including the IEEE TRANSACTIONS AND PATTERN RECOGNITION, and has authored 10 books and 200 journal papers. He is also a Croucher Senior Research Fellow and the Distinguished Speaker of the IEEE Computer Society, and fellow of the International Association for Pattern Recognition.